ELSEVIER

Journal of Molecular Catalysis A: Chemical 156 (2000) 267–274

JOURNAL OF MOLECULAR CATALYSIS A: CHEMICAL

www.elsevier.com/locate/molcata

Studies on anion promoted Titania 2: Preparation, characterisation and catalytic activity towards aromatic alkylation over sulfated titania

S.K. Samantaray [a,*], T. Mishra [b], K.M. Parida [a,1]

[a] *Regional Research Laboratory, Bhubaneswar 751013, Orissa, India*
[b] *NML, Field Station, Industrial Estate, Naroda, Ahmedabad 382330, India*

Received 30 July 1999; received in revised form 13 September 1999

Abstract

Sulfated titania samples with varying amounts of sulfate have been prepared by solid–solid kneading, as well as aqueous impregnation method, and are characterized using X-ray diffraction (XRD), FT-IR and N_2 adsorption–desorption isotherm. Surface area, average pore diameter and total pore volume are found to increase with the increase in sulfate content up to 7.5 wt.%, and thereafter decreases. Alkylation of aromatic compounds (benzene, toluene and chlorobenzene) with isopropanol is carried out in a fixed-bed flow reactor over these catalysts as a function of benzene to isopropanol molar ratio, reaction temperature, wt.% and source of sulfate ion. Among all the catalysts, the sample with 7.5 wt.% sulfate loading prepared from H_2SO_4 impregnation exhibits highest selectivity and yield towards alkylation of aromatic compounds to their corresponding isopropylated products.

Keywords: Sulfated titania; Aromatic compounds; Alkylation; Yield

1. Introduction

Catalyzed aromatic alkylation is a very important industrial process and would become even more so if the noxious homogeneous catalysts in current use, which are sources of pollution, industrial hazard and equipment corrosion [1–3], could be replaced by a noncorrosive solid acid catalyst. The alkylation of benzene with isopropanol or propylene to produce cumene is widely used in petrochemical industries because cumene is an important chemical intermediate mainly used for the production of phenol and acetone [4]. However, in general, alkylated benzene is in demand in chemical industry. In the recent year, attempts were made to replace the $AlCl_3$-based process with solid acid catalyst [5,6]. Wang et al. [7] and Kim et al. [8] studied mostly zeolite-based catalysts in the gas phase reactions due to its shape selective nature. Although these catalysts are used to catalyze the

* Corresponding author. Tel.: +91-674-581636; fax: +91-674-581637/581750.

E-mail addresses: kmparida@yahoo.com (S.K. Samantaray), kmparida@yahoo.com (K.M. Parida).

[1] Also corresponding author. Tel.: +91-674-581636; fax: +91-674-581637/581750.

1381-1169/00/$ - see front matter
PII: S1381-1169(99)00424-0

reaction, no major commercial process is yet in operation, due to the rapid aging of zeolite catalysts. Transition metal salts supported clay [9], solid phosphoric acid on silica [10] and calcined hydrotalcites [11] catalysts are also studied to catalyze this reaction.

It is also well documented that sulfated metal oxide can be used as solid acid catalyst due to their high acid strength. More recently, increasing application for these sulfated metal oxide solid acid are being found in heterogeneous catalysts, for a wide variety of applications, such as hydrocarbon isomerisation [12], nitration [13], reduction [14] and alkylation [15]. However, use of sulfated titania in these reaction is limited [16]. Moreover, it is well reported that the source sulfate ion and the method of preparation also play a significant role in the catalytic activity of the catalyst [16].

Therefore, in the present paper, we have attempted to study the physico-chemical behaviour and catalytic activity of sulfated titania prepared by different methods and varying the source of sulfate ion towards the gas phase alkylation of benzene and substituted benzenes using isopropanol as the alkylating agent.

2. Experimental

2.1. Materials and methods

Hydrated titania was precipitated at pH = 7 by adding 1:1 ammonia to the stirred aqueous solution of titanium tetrachloride. Obtained gel was filtered and washed repeatedly to remove Cl^- (negative $AgNO_3$ test), dried at 373 K, powdered and kept for the sulfate impregnation. A series of sulfated titania samples were prepared, using $(NH_4)_2SO_4$ as the source of sulfate ions, by solid–solid kneading method followed by slow heating at the rate of 283 K min^{-1} up to 773 K for 3 h. The other series of sulfated titania samples were prepared by aqueous impregnation method using dilute H_2SO_4. The suspended mass was evaporated to dryness on a hot plate while stirring, dried at 393 K and calcined at 773 K for 3 h in a muffle furnace.

3. Characterisation

3.1. Powder XRD

The XRD patterns of all the samples were recorded on a Philips (model: 1710) semiautomatic diffractometer using a Cu-K_α radiation source and Ni filter in the range of $2\theta = 6–70°$ at a scanning speed of 2° min^{-1}. The instrument was operated at 40 kV and 20 mA. The average crystallite size (L) of the particle was determined by XRD line broadening technique using a Scherrer equation,

$$L = 0.94\lambda / b\cos\theta \quad (1)$$

where λ is the wavelength of X-ray used and b is the relative peak broadening, calculated as $b^2 = b_{exp}^2 - b_{ref}^2$, where b_{exp} and b_{ref} are half-widths observed on a given sample and on a reference material, which is ideally crystalline, respectively.

3.2. FT-IR study

IR spectra of the samples were recorded with a Perkin-Elmer (model-Paragon 500) FT-IR spectrometer in the range of 4000–400 cm^{-1} on KBr phase. All the samples were degassed at 383 K in vacuum (1×10^{-4} Torr) before analysis.

3.3. Textural properties

Surface area (BET), total pore volume, average pore diameter, and pore size distribution were determined by the N_2 adsorption–desorption method at liquid nitrogen temperature using Quantasorb (Quantachrome, USA). Prior to adsorption–desorption measurements, the samples were degassed at 393 K at 10^{-4} Torr for 5 h.

3.4. Surface acidity

Surface acidity was determined spectrophotometrically on the basis of irreversible adsorption of organic bases (Fluka, Switzerland), such as pyridine (PY, $pK_a = 5.3$), morpholine (MOR, $pK_a = 8.3$), and piperidine (PP, $pK_a = 11.10$) [17]. In this method, adsorption experiment was carried out in a 50-ml stoppered conical flask taking 10 ml of each freshly prepared adsorbate solution, along with 50 mg of sample preheated at 393 K. The concentration range for each adsorbate was varied from 0.005 to 0.01 mol dm^{-3} in cyclohexane (Merk). While adsorption was taking place, the flasks were shaken constantly. After 2 h, the contents were filtered and absorbance of the filtrates was measured at preset wavelengths. For all cases, the sorption experiments were carried out in the adsorbate concentration range where Beer–Lambert's law is valid. The time required to reach equilibrium at 298 K was checked for all of the samples and was never found to take more than 1 h. All the absorbance measurements were carried out with a Chemito 2500 recording UV–visible spectrophotometer using 10-mm matched quartz cells.

The chemical interaction between the adsorbate and the sample may be described by the Langmuir adsorption isotherm,

$$C/X = 1/bX_m + C/X_m \quad (2)$$

where C is the concentration of organic substrate in solution in equilibrium with the adsorbed substrate, b is a constant, X is the amount of adsorbed substrate, and X_m is the monolayer coverage, which corresponds to the theoretical amount of solute required to cover all the active sites for base adsorption.

3.5. Catalytic activity

Alkylation of benzene and substituted benzenes with isopropanol were studied in a micropulse catalytic reactor (Sigma, India) with online GC. Prior to the reactions, all the catalysts were preheated in nitrogen atmosphere at 573 K for 1 h. The volume of each pulse (mixture of benzene or substituted benzenes and isopropanol) was maintained at 1 μl. Products were analysed by the gas chromatograph using 10-ft SS column with 10% TCEP.

4. Results and discussion

All the samples calcined at 773 K exhibit only anatase phase XRD pattern (Fig. 1), irrespective of the source and % of loading of sulfate ion. There is no indication of formation of titanium sulfate in any one of the samples; even in 10 wt.% SO_4^{2-} impregnation. To develop a better understanding of formation and crystallization in the presence of sulfate ion, the average crystallite size (L) perpendicular to the 210 plane was calculated from XRD patterns of pure titania, as well as sulfate modified titania, and is represented in Table 1. It shows that the crystallite size of titania decreases in the presence of sulfate ion, irrespective of the percentage of sulfate loading. This indicates that the crystallinity is more or less dependent on the presence of sulfate ion, but not on the percentage of sulfate loading. The crystallite size decreases in the presence of sulfate ions as SO_4^{2-} species could possibly interact with TiO_2 network and, thus, hinder the growth of the particle. Even a very small amount of SO_4^{2-} species is responsible for this effect. Therefore, the change in sulfate concentration did not change the crystallite size further. This type of effect is also observed in PO_4^{3-} [18,19] and WO_3 [20,21]. Therefore, it is assumed that the small amount of sulfate species is responsible for the lowering of crystallite size.

Infrared spectra of sulfated metal oxides generally show a strong absorption band at 1381 cm^{-1}, and broad bands at 1250–1100 cm^{-1} (Fig. 2). The 1381 cm^{-1} peak is the stretching frequency of S═O, and the 1250–1100 cm^{-1} peaks are the characteristic frequencies of SO_4^{2-}. The broad bands at 1250–1100 cm^{-1} resulted from the lowering of the symmetry in the free

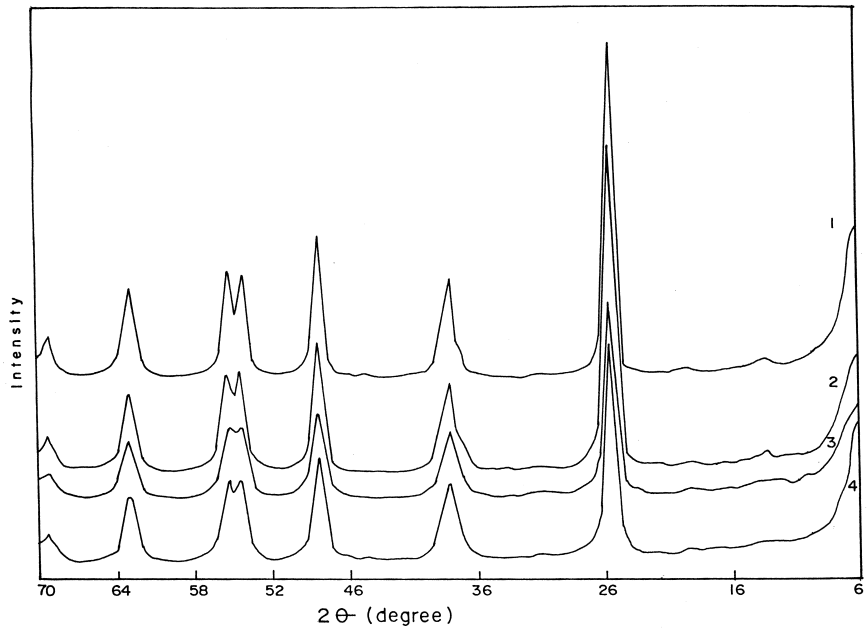

Fig. 1. Powder XRD patterns of sulfated titania samples (1) TiO_2, (2) $2.5SO_4^{2-}/TiO_2$, (3) $7.5SO_4^{2-}/TiO_2$, (4) $7.5SO_4^{2-}/TiO_2$ (H)*.

SO_4^{2-} (Td point group).When SO_4^{2-} is bound to the titania surface, the symmetry can be lowered to either C_{3V} or C_{2V} [22]. Here, the band that split into three peaks (1221, 1119, 1026 cm^{-1}) were assigned to the bidentately bound sulfate ion (C_{2V} point group). The bands at 1630 and 3430 cm^{-1} correspond to the bending and stretching of OH group of water molecules occluded in the sample, respectively.

It is observed that an increase in sulfate loading increases the surface area up to the sulfate loading of 7.5 wt.%. Further increase in sulfate loading to 10 wt.% resulted in a decrease in surface area (Table 1).

The trend remains the same irrespective of the source of sulphate ion. Similar trend is also maintained in case of the pore volume for both the series of materials. Therefore, the presence

Table 1
Textural parameters of sulfated titania
(H)* indicates H_2SO_4 impregnated samples.

Sample code	SO_4^{2-} (wt.%)	S_{BET} (m^2/g)	Total pore volume (cm^3/g)	Average pore diameter (Å)	Crystallite size (nm)
TiO_2	0	57.0	0.09	67.00	16.13
$2.5SO_4^{2-}/TiO_2$	2.5	73.9	0.13	61.78	7.08
$5.0SO_4^{2-}/TiO_2$	5.0	74.4	0.18	65.56	–
$7.5SO_4^{2-}/TiO_2$	7.5	94.5	0.22	74.56	6.8
$10.0SO_4^{2-}/TiO_2$	10.0	84.6	0.20	62.12	–
$2.5SO_4^{2-}/TiO_2$ (H)*	2.5	75.2	0.14	64.10	–
$5.0SO_4^{2-}/TiO_2$ (H)*	5.0	81.2	0.20	70.20	–
$7.5SO_4^{2-}/TiO_2$ (H)*	7.5	108.5	0.23	80.92	6.5
$10.0SO_4^{2-}/TiO_2$ (H)*	10.0	91.0	0.21	72.20	–

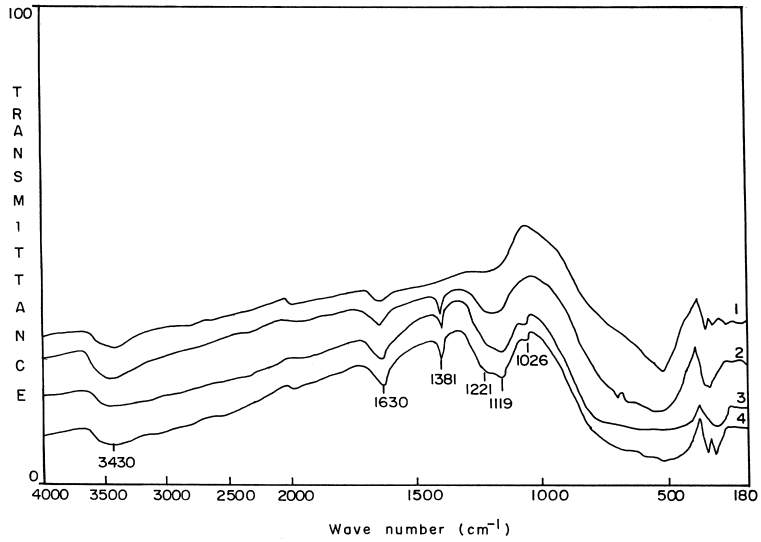

Fig. 2. FT-IR spectra of (1) TiO_2, (2) $2.5SO_4^{2-}/TiO_2$, (3) $7.5SO_4^{2-}/TiO_2$, (4) $7.5SO_4^{2-}/TiO_2$ (H)*.

of low amount of sulfate ion ($\leq$ 7.5 wt. %) may be responsible in the formation of porous network. It has been shown [12,23] that, in sulfated metal oxides, some of the hydroxyl bridges originally present in dried uncalcined and unsulfated titania replaced the sulfate ions. On calcination, the formation of oxy bonds takes place, and results in changes in the Ti–O–Ti bond strength due to attachment of the sulfate bridges.

Thus the changes in the Ti–O–Ti bond strength may be responsible for the formation of porous network. Consequently, the increase in surface area with an increase in sulfate loading up to 7.5 wt.% appears is due to the stabilizing effect of the sulfate ions. However, the plugging of more pores may have occured with higher sulfate loading resulting in a reduction of total pore volume to some extent and also decrease in surface area [12].

N_2 adsorption–desorption isotherm of all the samples are nearly of the same type, and can be included in the type IV or II of the BDDT classification [24], indicating the presence of mesopores in the material. Assuming the pores are cylindrical, the average pore diameter is calculated using the formula: $d = 4V_p/S_p$, where, d is the average pore diameter, V_p is the pore volume, and S_p is the specific internal surface area of the pores. Average pore diameter is found to be in the same range, irrespective of sulfate concentration and source of sulfate ion. This is also supported by the mesopore size distribution curve (Fig. 3), calculated by BJH equation [25].

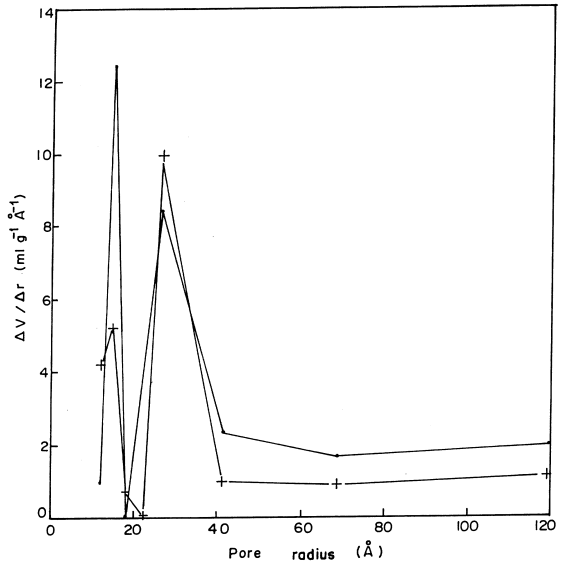

Fig. 3. Distribution of pore size as a function of pore radius of (.) $7.5SO_4^{2-}/TiO_2$, (+) $7.5SO_4^{2-}/TiO_2$ (H)*.

Table 2
Acid sites of sulfated titania samples
(H)* indicates H_2SO_4 impregnated samples.

Sample	SO_4^{2-} (wt.%)	Acidity (μmol/gm)		
		PP ($pK_a = 11.1$)	MOR ($pK_a = 8.33$)	Py ($pK_a = 5.3$)
TiO_2	0	220	182	120
$2.5SO_4^{2-}/TiO_2$	2.5	382	287	225
$5.0SO_4^{2-}/TiO_2$	5.0	485	322	233
$7.5SO_4^{2-}/TiO_2$	7.5	622	425	280
$10.0SO_4^{2-}/TiO_2$	10	443	341	205
$7.5SO_4^{2-}/TiO_2$ (H)*	7.5	681	522	303
$10.0SO_4^{2-}/TiO_2$ (H)*	10.0	455	345	221

The total acidity measured by the adsorption of PP, strong acid sites by PY, and moderate acid sites by MOR, gradually increased with increased sulfate loading of up to 7.5 wt.%, and thereafter decreases on further addition (Table 2). This indicates that all types of acid sites are present in SO_4^{2-}/TiO_2. The initial increase in surface acidity, with an increase in sulfate loading of up to 7.5 wt.%, may be due to sulfate monolayer formation. The decrease in the surface acidity at high sulfate concentrations is probable due to the formation of polysulfate, which decreased the number of Brönsted sites and consequently that of total acid sites [12]. It is observed that sulfated samples prepared using sulfuric acid exhibit higher acidity compared to the samples prepared using $(NH_4)_2SO_4$. It is reasonable to assume that during the preparation procedure, the aqueous sulfuric acid protonates all types of titania hydroxyls by an acid-base reaction:

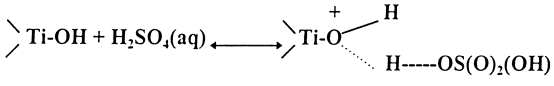

However, sulfate of ammonium sulfate by solid–solid kneading method undergoes interaction with all types of basic hydroxyls to a smaller extent resulting in less acidity compared to sulfate of sulfuric acid by aqueous impregnation method. Similar observations have been reported earlier in case of SO_4^{2-} [26] and PO_4^{3-} [27] on alumina.

From the preliminary study, it was found that 7.5 wt.% sulfate-loaded samples of both the series exhibit highest conversion of benzene to cumene. The highest conversion may be due to its high surface area. So, for a detailed investigation, only 7.5 wt.% sulfate-loaded samples were used. Alkylation of benzene with isopropanol was studied at various benzene to isopropanol molar ratio with varying temperatures in the range 453–523 K. Benzene conversion increases with the increase in temperature

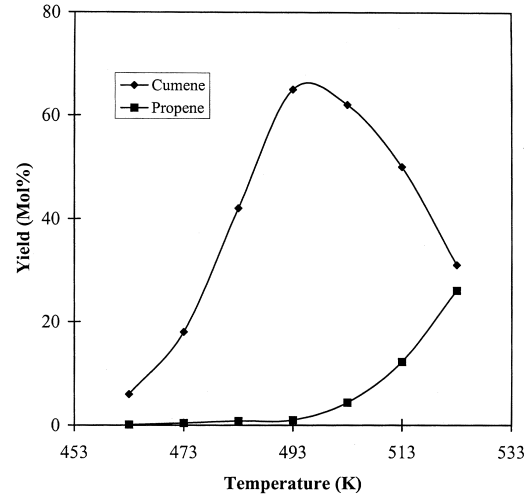

Fig. 4. Variation of product selectivities of alkylation of benzene with respect to temperature over $7.5SO_4^{2-}/TiO_2$ (H)* at benzene to isopropanol molar ratio of 10.

up to 493 K, and thereafter decreases (Fig. 4). However, the isopropanol conversion increases with the increase in temperature even above 493 K.

Fig. 4 indicates that the propene formation is very low within 493 K, but suddenly increases after reaching 493 K. This implies that above 493 K, isopropanol directly dehydrates to propene, thus, decreasing the cumene formation. Benzene to isopropanol molar ratio also plays an important role in deciding the product selectivity (Fig. 5). Particularly, the product selectivity was found to be highest at the benzene to isopropanol molar ratio of 10.

The catalytic behaviour of sulfated titania towards the Friedel–Crafts alkylation reactions was also studied by a series of substituted benzenes (Fig. 6). Interestingly, it was found that the alkylation is highest with benzene and lowest with chlorobenzene. In general, methyl substitution enhances the rate of alkylation reaction. So, with toluene, highest conversion is expected than with benzene. However, we found the reverse order; the yield of alkylated product, in the case of benzene, is slightly higher than toluene over the sulfated catalysts. Mostly, the toluene alkylation gives the *para* substituted product, which may be due to the steric factor, thus prohibiting the *ortho* substitution. This is

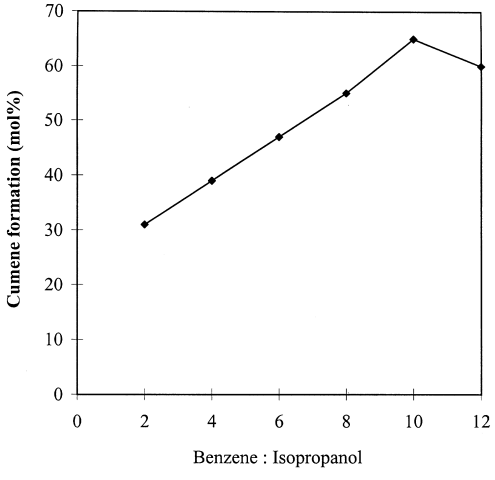

Fig. 5. Effect of benzene to isopropanol molar ratio on the cumene formation over $7.5SO_4^{2-}/TiO_2$ (H)* at 493 K.

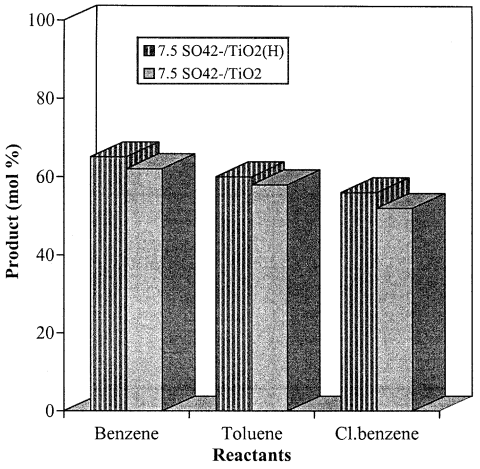

Fig. 6. Variation in alkylated product with the variation in reactants over both the sulfated titania prepared from different methods.

because the rate of toluene alkylation seems to be limited in medium-pore catalyst by reagent diffusion inside the crystal volume. If this is true, the extent of alkylation (% of conversion) will depend on the diffusion coefficient of aromatic hydrocarbon, and should follow the order [28]: benzene > toluene > *p*-xylene > ethyl benzene > *m*-xylene > *o*-xylene.

5. Conclusions

In the alkylation of benzene with isopropanol, sulfated titania prepared from sulfuric acid showed better activity and selectivity over titania modified with ammonium sulfate. The decrease in the yield of alkyl-substituted benzene above 493 K is the consequence of the preferential dehydration of isopropanol over alkylation reaction. Catalytic proficiency was found to be dependent on sulfate ion concentration in the catalyst, and on the benzene to alcohol molar ratio.

Acknowledgements

The authors are thankful to Prof. H.S. Ray, Director, Regional Research Laboratory,

Bhubaneswar and Prof. P. Ramachandra Rao, Director, NML, Jamshedpur for their permission to publish this paper, and to Dr. S.B. Rao, Head, IC Division, for his constant encouragement throughout this work.

References

[1] G. de Almeida, J.L.M. Dufaux, Y. Ben Taarit, C. Naccache, Appl. Catal. A 114 (1994) 141–159.
[2] G.A. Olah, Friedel–Crafts Chemistry, Wiley, New York, 1973.
[3] H. Miki, US Pat. 4 347 393, 1982.
[4] P.R. Pujado, J.R. Salazav, C.V. Berger, Hydrocarbon Process. 55 (1976) 91.
[5] N.Y. Chen, Catal. Rev.-Sci. Eng. 28 (1986) 185.
[6] SRI International, PER Report 33C, March 1993.
[7] I. Wang, C. Ag, B.J. Lee, M.H. Chen, Appl. Catal. 54 (1989) 257.
[8] J.H. Kim, S. Namba, T. Yashima, in: H.G. Karge, J. Weitkan (Eds.), Zeolites Catalysts, Sorb and Detergent Builders, Elsevier, Amsterdam, 1988, p. 71.
[9] J.H. Clark, A.P. Kybett, D.J. Macquarrie, S.J. Barlow, P. Landon, J. Chem. Soc., Chem. Commun. (1989) 1553, (in part).
[10] E.K. Jones, D.D. Dettner, US 173, 1958.
[11] S. Velu, C.S. Swamy, Appl. Catal. 119 (1994) 241.
[12] A.K. Dalai, R. Sethuraman, S.P.R. Katikaneni, R.O. Idem, Ind. Eng. Chem. Res. 37 (1998) 3869.
[13] K.M. Parida, P.K. Pattnayak, Catal. Lett. 47 (1997) 255.
[14] J.P. Chen, R.T. Yang, J. Catal. 139 (1993) 277.
[15] G.D. Yadav, T.S. Thorat, P.S. Kumbhar, Tetradedron Lett. 34 (1993) 529.
[16] A. Hess, E. Kemnitz, Appl. Catal. A 149 (1997) 373.
[17] J.M. Campelo, A. Garcia, J.M. Guterrez, D. Luna, J.M. Mrinas, J. Colloid Interface Sci. 95 (1983) 544, and references therein.
[18] K. Kandori, S. Uchida, S. Kataoka, T. Ishikawa, J. Mater. Sci. 27 (1992) 719.
[19] K.M. Parida, M. Acharya, S.K. Samantaray, T. Mishra, J. Colloid Interface Sci. 217 (1999) 388.
[20] D.G. Barton, S.L. Soled, G.D. Meitzner, G.A. Fuentes, E. Iglesia, J. Catal. 181 (1999) 57.
[21] L.J. Alemany, M.A. Larrubia, M.C. Jimenez, F. Delgado, J.M. Blasco, React. Kinet. Catal. Lett. 60 (1) (1997) 41.
[22] K. Nakamoto, Infrared and Raman Spectra of Inorganic and Coordination Compounds, 4th edn., Wiley, New York, 1986.
[23] B.H. Davis, R.A. Keogh, R. Srinivasan, Catal. Today 20 (1994) 219–256.
[24] S. Brunauer, D.W. Demming, L.S. Demming, E. Teller, J. Am. Chem. Soc. 62 (1940) 1723.
[25] E.P. Barrett, L.G. Joyner, P.P. Halonda, J. Am. Chem. Soc. 73 (1951) 373.
[26] Y. Okamoto, T. Imanaka, J. Phys. Chem. 92 (1988) 7102.
[27] J.M. Lewis, R.A. Kydd, J. Catal. 132 (1991) 465.
[28] N.V. Choudary, R.V. Jasva, S.G.T. Bhat, T.S.R. Prasad Rao, Zeolites: facts, figures, future, in: Stud. Surf. Sci. Catal. Vol. 49(B) Elsevier, Admsterdam, 1989, p. 867.